

SSC CENTRAL DESIGN GROUP
LAWRENCE BERKELEY LABORATORY
BERKELEY, CALIFORNIA 94720

November 5, 1988

FINITE ELEMENT ANALYSIS OF THE NC-9 DIPOLE

Note #2

Prestressed Assembly Loading

M. Chapman and B. Wands

INTRODUCTION

In this report, which is second in a series on a finite element analysis of the NC-9 dipole, stresses and deflections of the dipole after collaring are examined.

The collaring operation, in which the collars halves are brought together around the pre-fabricated coils and interlocked together by inserted keys (Figure 1), produces compressive azimuthal stresses in the coils, and tensile azimuthal stresses in the collars as a result of the designed interference between the coils and the collars. This compressive prestress of the coils is important in preventing coil motion during magnet energization that might degrade the magnetic field or initiate a quench of the magnet. The amount of prestress developed in the coils varies from magnet to magnet and depends primarily on the initial coil size, the curing history of the coil, and the amount of shimming material placed between the coils and the collars at the poles. The pole shims (Figure 2) are chosen separately for each set of coils so that the amount of prestress developed in the coils can be controlled. In this analysis, the stresses and deflections for a typical magnet with inner coil prestress of 8500 psi and outer coil prestress of 6600 psi are calculated.

DESCRIPTION OF MODEL

The calculation uses a 2-D model of the NC-9 cross-section, which is described in detail in the first note in this series.¹ Briefly, the model consists of inner and outer coils modeled with individual conductors and wedges, aluminum collar laminations, tapered keys, and pins that align successive collar laminations. By modeling two successive laminations in the same plane (labeled "front collar" and "back collar", Figure 1) and using appropriate boundary conditions, only one quadrant of the cross-section need be modeled. The ANSYS finite element code was used for this analysis.

The mechanical and material properties of the coil are non-linear, inelastic, and orthotropic. At this point it is not practical to accurately model these properties, and it is necessary to make simplifying assumptions about the coil behavior. For this analysis, the coils are assumed to be elastic, linear and isotropic. In an effort to determine the sensitivity of the calculations to these assumptions, three coil parameters are varied in the following ways, and the effects on the results are examined:

1. Coil Young's modulus (E_{coil}): This was either 1.5×10^6 psi or 0.75×10^6 psi
2. Coil planar behavior assumption: This was either plane strain or plane stress
3. Interaction between adjacent conductors: This was either frictionless sliding or fully coupled

It is assumed in all cases that the coil elastic coefficients (Young's modulus, Poisson's ratio ($\nu = .3$), and shear modulus) are invariant with stress, and that coils are free to slide with respect to each other and the collars.

DESCRIPTION OF LOADING

We wish to load the model such that an average azimuthal prestress of 8500 psi is developed in the inner coil and an average azimuthal prestress of 6600 psi is developed in the outer coil. Although there are many different ways to load the finite element

model as it has been created, for our purposes it will serve to examine two types of midplane loading of the coil (see Figure 3):

1. Uniform pressure loading: uniform pressures are applied to the coil midplanes equal to 8500 psi for the inner coil and 6600 psi for the outer coil.
2. Uniform displacement loading: uniform vertical displacements are applied to the individual coil midplanes such that the *average* stress at the midplane is 8500 psi for the inner coil and 6600 psi for the outer coil. The displacements are uniform across each coil midplane; however, different displacements are applied to the inner coil than those applied to the outer coil.

RESULTS

The vertical and horizontal diametral deflections of the collars are listed in Table 1 for the different coil models studied and the different loadings applied to the coils. The typical deflections of the front collar and back collar are shown in Figures 4 & 5 respectively, and the relative motion of successive collar laminations are shown in Figure 6. Typical contours of von Mises's stress are shown in Figures 7 & 8 for the front and back collars, respectively.

Contours of azimuthal stress for the inner and outer coils are shown for Model 1 in Figures 9 & 10 for the uniform pressure and uniform displacement loadings respectively. These stress patterns are typical for Models 1-3, in which the conductors are not free to slide relative to each other. Coil stress contours for Model 4 are shown in Figures 11 & 12 for the uniform pressure and uniform displacement loadings. These contours are typical for Models 4 & 5 in which the conductors are permitted to slide freely with respect to each other. The azimuthal coil stress at the poles and midplanes for uniform displacement loading at the midplane are shown in Table 2. The stresses are resolved into their linearized membrane and bending equivalents. The sum and difference of these two components result in the stress at the inner and outer edges of the coils, which are also listed in Table 2. The relationship between these linearized

quantities and the actual stress distribution is shown graphically in Figures 13-16 for Model 1.

Figure 17 shows typical conductor/conductor relative motion for Models 4 & 5 in which the conductors are free to slide.

DISCUSSION

Collar Deflections and Stresses

The calculated change in vertical collar diameter is 0.029–0.030 in, which compares well with the 0.029–0.035-in. measurements made on actual dipoles,² noting that the actual coil prestress varies from magnet to magnet. The calculated diameter change is virtually invariant with the coil properties specified in the model which indicates that in the vertical direction the assembly behaves nearly as two springs in series. That is, provided the load remains constant, and the distribution of the load from the coil to the collar does not vary significantly, the collar vertical deflection will be constant. The horizontal change in collar diameter varies from 0.001–0.002 in. which again compares well with the measured values of 0–0.005 in.

Other collar geometry changes of interest can be seen in Figure 6. There is relative rotation between the front and back collars which is evident at the tab at the top of the collar. This rotation is on the order of .003 in and compares well with field measurements on actual magnets. This rotation causes the back collar to pull away from the outer coil at the pole so that only the front collar is in contact with the coil along this surface. This phenomena has been verified by examining a "cookie" cross-section from Magnet F-1, and by tests with pressure-sensitive "Fuji" paper performed at LBL.³

Examination of a "cookie" cross-section also provides verification of the deflections at the keyways and at the tang/back collar region noted on Figure 6. In addition, it is evident from the "cookie" cross-section that the tang contacts the back collar at point A indicated on Figure 6; the model predicts the same contact point.

The collar stresses are shown as contours of von Mises's stress in Figures 7 & 8 for the front and back collars, respectively. These calculated values should be compared with the yield strength of 7075-T6 aluminum which is 73,000 psi.⁴ Areas of high stress occur at the keyways, at the outer pole of the front collar, and near the hole in the front collar. The element mesh for the collars is not sufficiently dense to accurately calculate stress concentrations, and the peak stresses calculated in these areas should be ignored. Nonetheless, there is a evidently a significant area of the collar which experiences equivalent stresses in excess of 50,000 psi which is fully 2/3 of the yield strength of the material. It should also be considered that these collar stresses correspond to a inner coil prestress of 8500 psi and an outer coil prestress of 6600 psi which do not represent upper limits on these quantities. Peak coil stresses 50% greater than those considered here would be likely to cause significant yielding of the collars and result in permanent deformation.

A first order verification of the calculated collar stresses can be obtained by comparing the average azimuthal (or membrane) stress of the collars through any section, to the applied loads to the coils. In this case, the applied load per unit depth is the azimuthal stress on the coils multiplied by the area of the coils. For the inner coil:

$$F_{\text{inner}} = \sigma_{\text{inner}} \times A_{\text{inner}} = 8500 \text{ psi} \times (.390\text{''})(1\text{''}) = 3315 \text{ lb}$$

$$F_{\text{outer}} = \sigma_{\text{outer}} \times A_{\text{outer}} = 6600 \text{ psi} \times (.420\text{''})(1\text{''}) = 2772 \text{ lb}$$

$$F_{\text{applied}} = F_{\text{inner}} + F_{\text{outer}} = 6087 \text{ lb}$$

This applied force must be reacted by the average membrane stress of the collars through any section. For this comparison, a section through the collars is taken at A-A on Figures 7 & 8, through which the average membrane stress is calculated to be:

$$\sigma_{\text{memb)front}} = 23880 \text{ psi}$$

$$\sigma_{\text{memb)back}} = -2970 \text{ psi}$$

$$\sigma_{\text{memb)total}} = 23880 \text{ psi} - 2970 \text{ psi} = 20910 \text{ psi}$$

which produces a reaction force

$$F_{\text{reaction}} = \sigma_{\text{memb)total}} \times A_{\text{collar}} = 20910 \text{ psi} \times (.558\text{''})(.5\text{''}) = 5834 \text{ lb}$$

where the (.5") results from the fact that each collar has a depth of .5" whereas the coils have a depth of 1". The agreement between F_{applied} and F_{reaction} is within 5%, suggesting that from a force-balance point-of-view, the calculated collar stresses seem reasonable.

Coil Deflections and Stresses

The material and mechanical properties of the coil, as well as the unstressed dimensions of the coil, represent the largest uncertainty in this analysis. It has been shown that for prestress loads, the collar reactions are largely insensitive to the coil property and loading assumptions. This is not true for the coil reactions.

The coils have been modeled as linear, elastic and isotropic, whereas in actuality they are none of these. Measurements have shown that the azimuthal stress/strain behavior is non-linear, with a very low modulus at low stresses increasing to a modulus of $0.75\text{--}1.5 \times 10^6$ psi at stresses higher than 3000 psi. In effect, the unstressed coil is somewhat "spongy," and because of this, it is difficult to determine the initial conditions of the coil prior to collaring. At higher stresses, however, the stress/strain behavior of the coil becomes more linear. The azimuthal coil modulus is also a function of radius, with the modulus at the inner edge of the coils being higher than that at the outer edge. This is thought to be the result of the keystoneing of the conductor, as well as the uneven distribution of the fiberglass/epoxy composite after coil curing. Little is known about the behavior of the coil in shear, or its behavior in the axial and radial directions. The sensitivity of the coil stress results to some of these coil parameters has been reported on separately in the third paper in this series⁵ and is significant in many cases. Efforts are underway to measure many of these parameters; however, currently, they are not sufficiently specified to allow calculation of the stress state of the coils given only their initial dimensions. Therefore, the calculated coil stresses must be interpreted qualitatively, rather than quantitatively.

A qualitative comparison of uniform pressure loading and uniform displacement loading reveals that the stresses at the coil midplanes are very sensitive to small changes in the coil profile at the midplanes. This can be seen in Figures 9 & 10 which

show contours of azimuthal stress for Model 1 with uniform pressure loading and uniform displacement loading, respectively. In Figure 10, the stress at the inner coil midplane varies from 13300 psi at the inner edge to 3700 psi at the outer edge. When the same model is loaded with uniform pressure (Figure 9), the stresses across the midplane are by definition uniform, and the vertical displacement profile at the inner coil midplane is linear with the displacement at the outer edge .0025" higher than that at the inner edge. The nominal width of the inner coil is .390 in, therefore, a change in the midplane profile of only .37 degrees produces a stress gradient with the ratio of inner edge to outer edge stresses greater than 4:1. This high sensitivity of the midplane stresses is a phenomena common to thick cylindrical sections. Figure 18 shows a section of a thick cylinder with the same inner and outer radii as the inner coil in a rigid cavity loaded with uniform midplane displacements. The azimuthal stress patterns are similar to those of the inner coil, and the gradient is actually worse than that calculated for the coil.

The sensitivity of the midplane stresses to the midplane profile will depend on the coil azimuthal modulus, its variation with radius and the shear stiffness of the coil. For models in which the coil azimuthal stiffness has been reduced (either by lowering the Young's modulus or by modeling the coil in plane stress) the stress gradients are less severe. This can be seen by comparing the magnitudes of the bending stress listed in Table 2 for the different models. The stress gradients are also reduced for models in which the shear stiffness of the coils has been reduced by allowing individual conductors to slide freely (compare Figures 11 & 12 which indicate azimuthal coil stress for Model 4 for uniform pressure loading and uniform displacement loading, respectively).

Figure 10 reveals a very high stress gradient at the outer coil pole. The cause of this gradient in the model is a combination rotation/bending of the front collar in the region of the outer coil pole. This rotation and bending can be seen qualitatively in Figure 6 which show collar displacements and quantitatively in Figure 19 which plots the deflections of the outer pole surfaces for the front and back collar. The deflections plotted are normal to the face of the outer pole. A collar displacement purely normal to the pole would appear as a straight line on this plot, and therefore, there is a combination rotation and bending of the outer pole region of the front collar of .003."

Thus, the displacement profile here is similar to those examined at the coil midplanes, and the effects on the coil stress are the same.

It must be remembered that because of the uncertainties in the coil parameters previously mentioned, the stress patterns calculated here can only be considered relatively. In other words, the stress gradients discussed above may or may not exist and may even be in the other direction in actual dipoles. The calculation, however, indicates that the stress state of the coil near the poles and the midplane is very sensitive, and can be changed substantially by small perturbations in the coil profile at these areas.

A few comments on the sliding conductor model versus the fixed conductor model. The coils consist of many conductors each consisting of stranded cable wrapped first with Kapton tape and second with epoxy impregnated fiberglass tape. The coil curing process cures the epoxy/fiberglass composite and binds adjacent conductors together. This would seem to favor the idea of modelling the conductors as fixed together as opposed to free to slide. Nevertheless, small amounts of sliding ($\approx .001$) might occur between the stranded cable and the Kapton wrapping, and so it is useful to compare the two coil models. To the first order, the roman arch configuration of the coils with the keystone cables is an inherently stable structure for this loading in that no conductor/conductor frictional forces are required to hold the structure together. However, small relative sliding does occur between conductors, with the largest values of .001-.002" occurring between the wedges and adjacent conductors (see Figure 17). These values are typical for all runs in which the conductors were allowed to slide freely. The wedges represent a geometrical discontinuity of sorts, and it is conceivable that they represent preferred slip planes of the structure. This idea is reinforced by an examination of the shear stresses between conductors and wedges for Model 1 (conductors *not* permitted to slide) in Figure 20 which shows that the maximum shear stresses (absolute value) are also developed between the wedges and adjacent conductors for the inner coil.⁶

CONCLUSION

The consistency of the calculated collar deflections with experimental measurements and observations indicate that the finite element model accurately models the mechanical response of the collars, including the subtle interactions between successive collar laminations through the pins and keys. The stresses developed in the collars are below the yield stress of the collar material for the coil prestress examined (with the possible exception of a few small areas of stress concentration), however, peak loadings experienced by the collars during assembly may be sufficient to induce permanent deformation.

The response of the collars to a given assembly prestress load is shown to be largely independent of the coil assumptions made, however, this is not the case for the calculated coil stresses. Although it is not possible at this point to calculate the stress distribution in the coil with confidence, it is possible to show that the stress distribution at the coil midplanes and poles is highly sensitive to the exact coil profile at these points. Finally, a comparison of coil models in which adjacent conductors are fixed together, to coil models in which adjacent conductors are permitted to slide freely with respect to each other, indicates that the sharp angular transition created by the wedges causes the maximum relative sliding and shear force between conductor/conductor and conductor/wedge interfaces to occur at the wedge locations.

ENDNOTES

- 1 Wands RH and Chapman MS, Finite Element Analysis of NC-9 Dipole, Note 1, Model Description, B. Wands and M. Chapman. SSC-N-530, May 1988.
- 2 LBL Prompt reports: D-15A series of magnets.
- 3 June MSIM meeting, presentation by Clyde Taylor of "Fuji" paper experimental results.
- 4 Mark's Standard Handbook for Mechanical Engineers, 9th ed., p 6-78.
- 5 Wands RH, Chapman MS: Finite Element Analysis of the NC-Dipole, Note #3, Dependence of Coil Azimuthal Stress on Material Properties, Planar Behavior Assumption, and Midplane Displacements. SSC-N-???, Oct 1988.
- 6 The shear stresses plotted are in element coordinate systems (ELEM CS), which in this case have x axes along the conductor/conductor or conductor/wedge interface and have y axes orthogonal to the interfaces. Therefore, the shear stresses indicated in Figure 20 are along the conductor/conductor or conductor/wedge interface and represent the shear stress necessary to prevent conductor sliding.

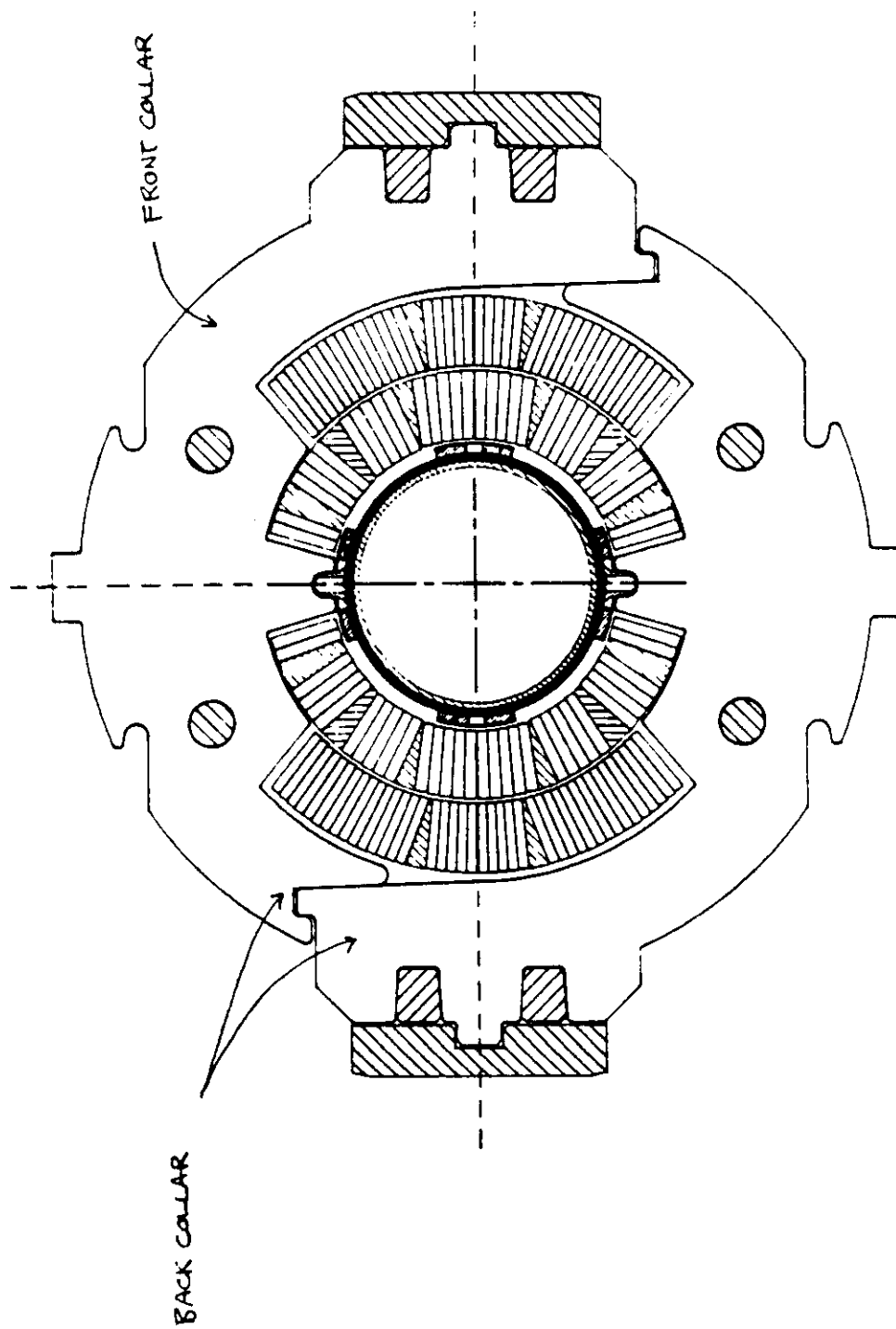
Table I. Collar Deflections

	Model Number				
	1	2	3	4	5
Coil Modulus (psi)	1.5x10 ⁶	0.75x10 ⁶	0.75x10 ⁶	1.5x10 ⁶	0.75x10 ⁶
Conductors free to slide or fixed	fixed	fixed	fixed	free	free
Coil Plain strain or plain stress	strain	strain	stress	strain	strain
Uniform Midplane Pressure Loading					
Vertical diameter change (in.)	0.028	0.029	0.029	0.029	0.029
Horizontal dia. change (in.)	0.002	0.002	0.002	0.002	0.002
Uniform Midplane Displacement Loading					
Vertical diameter change (in.)	0.029	0.030	0.030	0.029	0.029
Horizontal dia. change (in.)	0.001	0.001	0.001	0.002	0.002

Table 2. Coil Stresses

	Model Number				
	1	2	3	4	5
Coil Modulus (psi)	1.5x10 ⁶	0.75x10 ⁶	0.75x10 ⁶	1.5x10 ⁶	0.75x10 ⁶
Conductors free to slide or fixed	fixed	fixed	fixed	free	free
Coil Plain strain or plain stress	strain	strain	stress	strain	strain
Inner Coil Midplane					
Membrane	-8511	-8510	-8533	-8533	-8532
Bending	-4796	-4171	-4478	-2686	-2824
Inner radius	-13310	-12680	-13010	-11220	-11360
Outer radius	-3715	-4340	-4055	-5846	-5708
Inner Coil Pole					
Membrane	-8512	-8432	-8408	-8580	-8520
Bending	-1617	-504	-236	141	317
Inner radius	-10130	-8935	-8640	-8439	-8203
Outer radius	-6895	-7928	-8169	-8721	-8837
Outer Coil Midplane					
Membrane	-6627	-6648	-6661	-6481	-6503
Bending	-3411	-3322	-3555	0	-510
Inner radius	-10040	-9969	-10220	-6481	-7014
Outer radius	-3216	-3326	-3106	-6481	-5993
Outer Coil Pole					
Membrane	-6196	-6170	-6150	-6268	-6285
Bending	5811	3833	3630	3052	1649
Inner radius	-385	-2337	-2519	-3215	-4636
Outer radius	-12010	-10000	-9780	-9320	-7933

Figure 1 SSC NC-9 Dipole Cross-section



SSC DIPOLE X-SECTION
w/ LBL NC-9 COIL

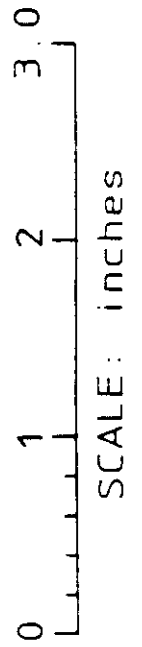
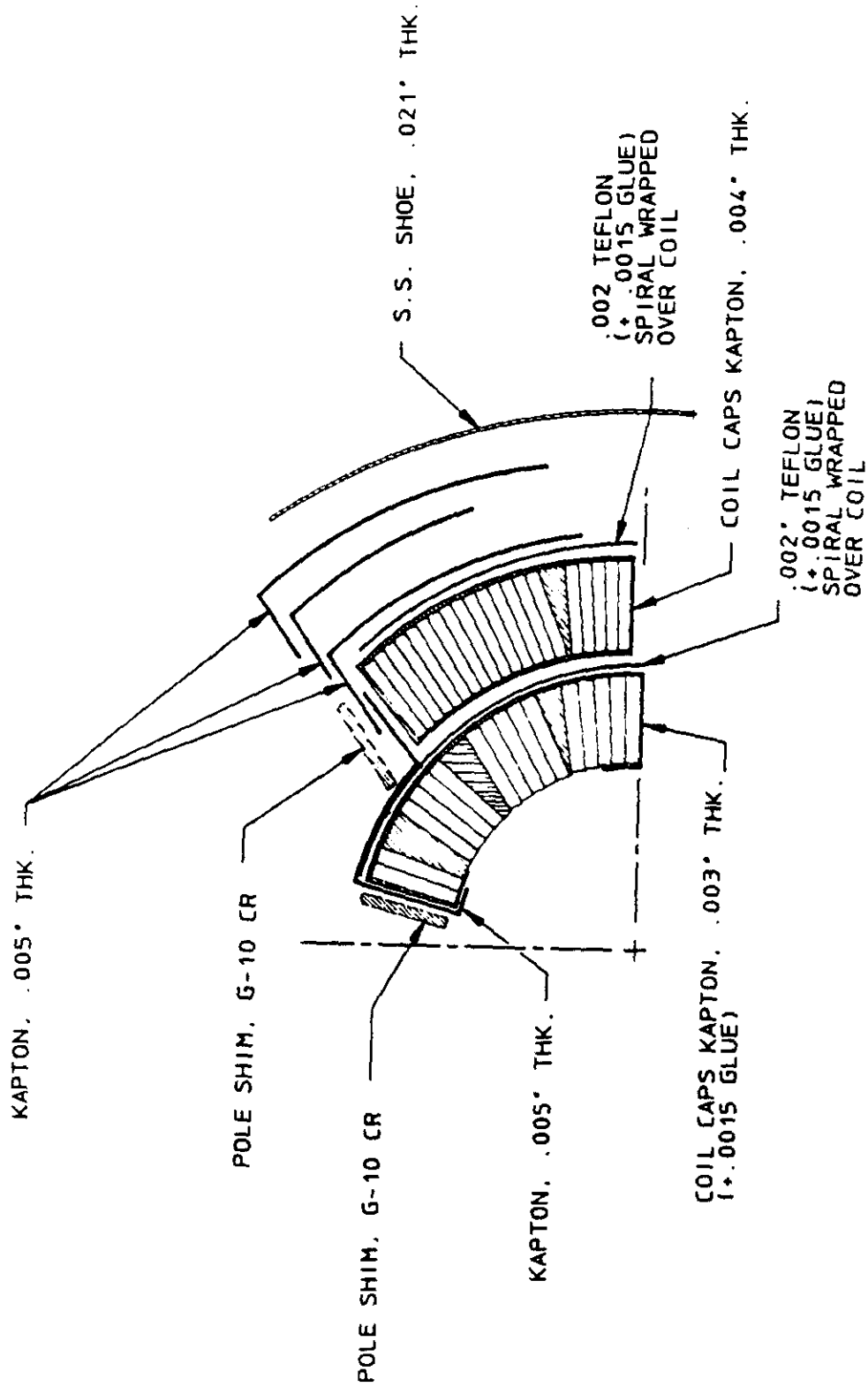


Figure 2 Exploded View of Coil Quadrant
Showing Pole Shims

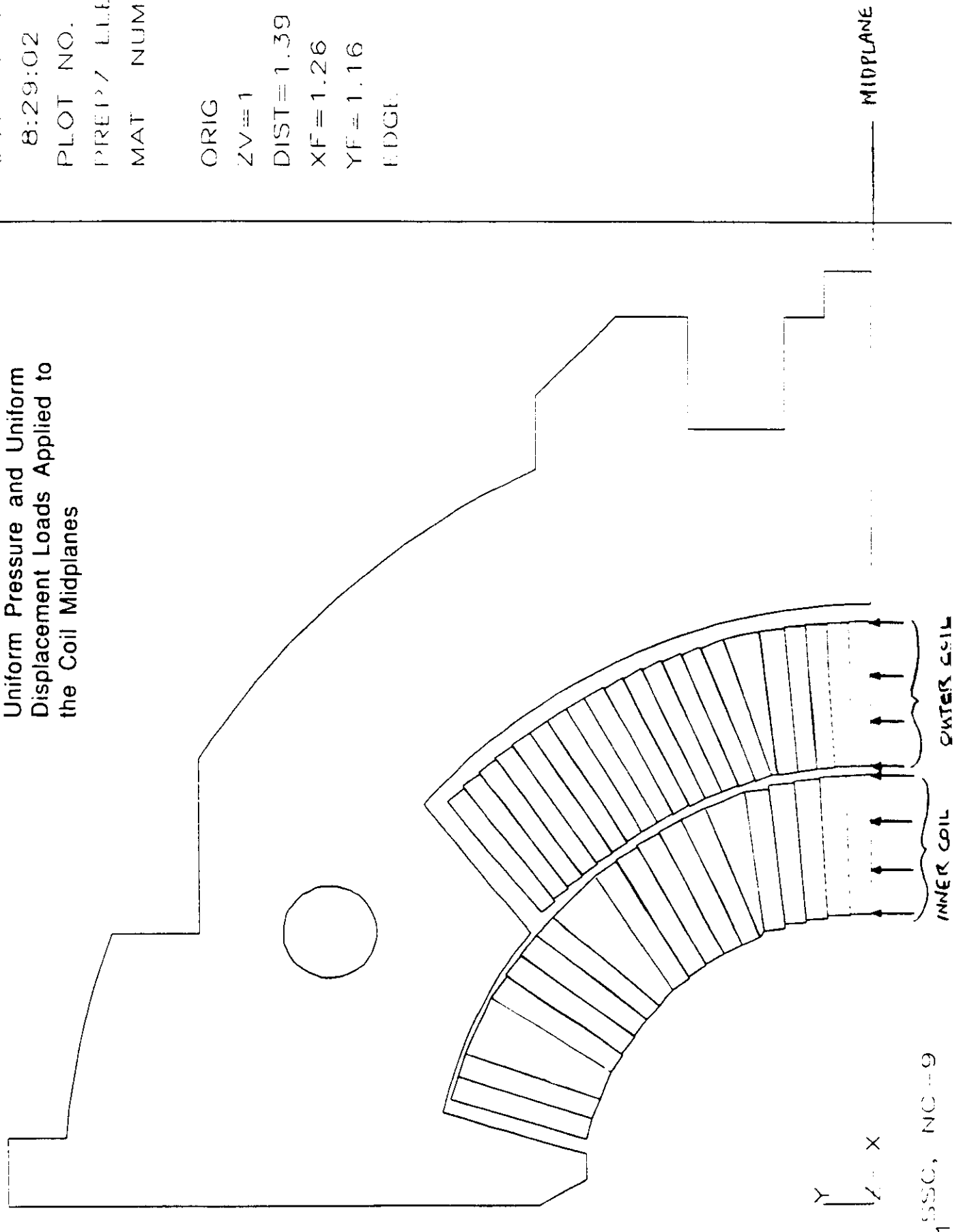


EXPLODED VIEW
COIL QUADRANT-NO SCALE
(COLLAR REMOVED FOR CLARITY)

ANSYS 4.1.5
 OCT 7 1988
 8:29:02
 PLOT NO. 1
 PREP7 LLEMENT1,
 MAT NUM

ORIG
 ZV=1
 DIST=1.39
 XF=1.26
 YF=1.16
 EDGE

Figure 3 Location and Direction of Uniform Pressure and Uniform Displacement Loads Applied to the Coil Midplanes



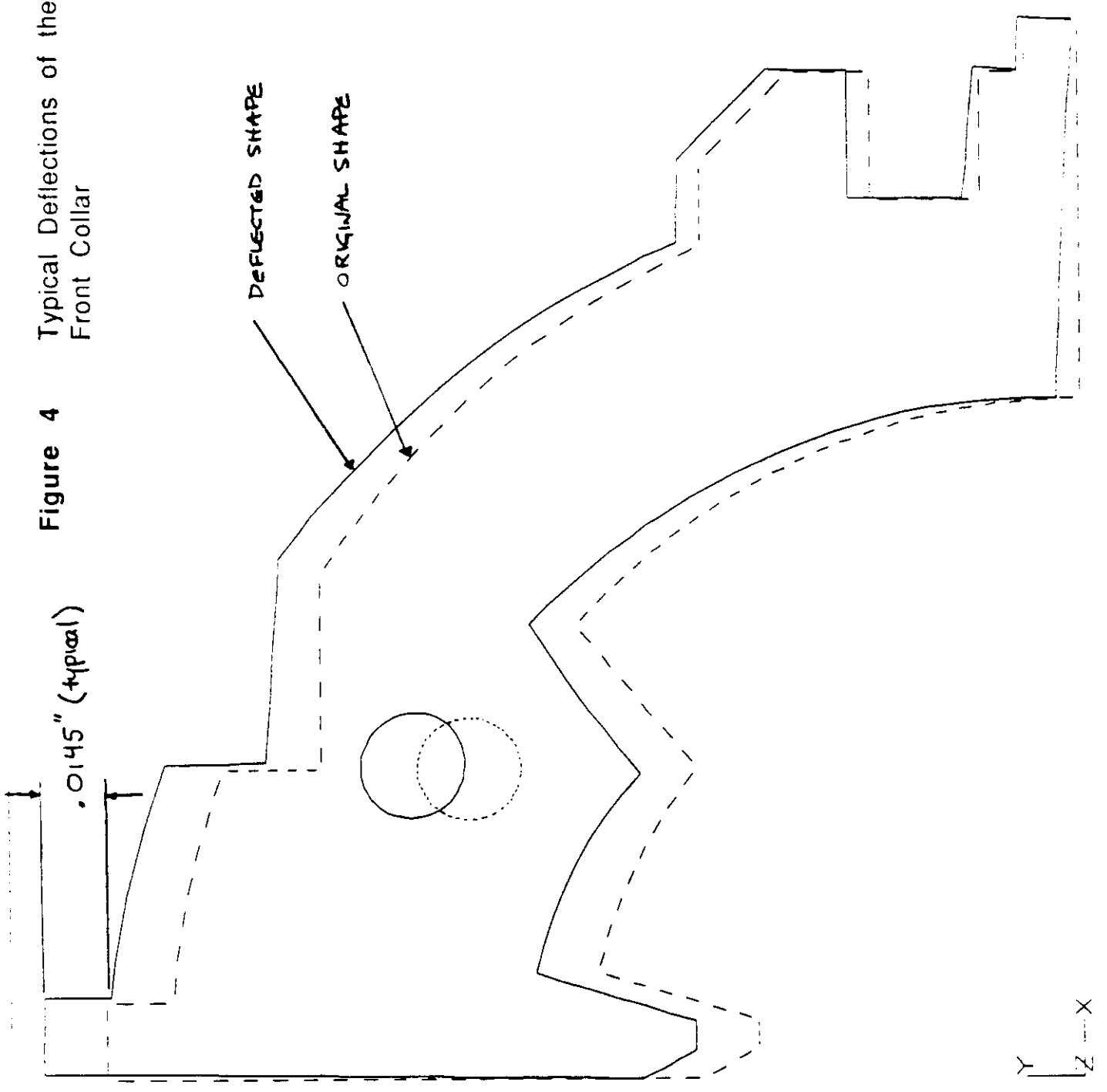


Figure 4 Typical Deflections of the Front Collar

ANSYS 4.3
 OCT 6 1988
 9:10:38
 PLOT NO. 2
 POS11 DISPL.
 STEP=2
 IIR=15

ORIG
 ZV=1
 DIST=1.39
 XF=1.26
 YF=1.16
 EDGE
 DMAX=.0151
 * DSCA=10

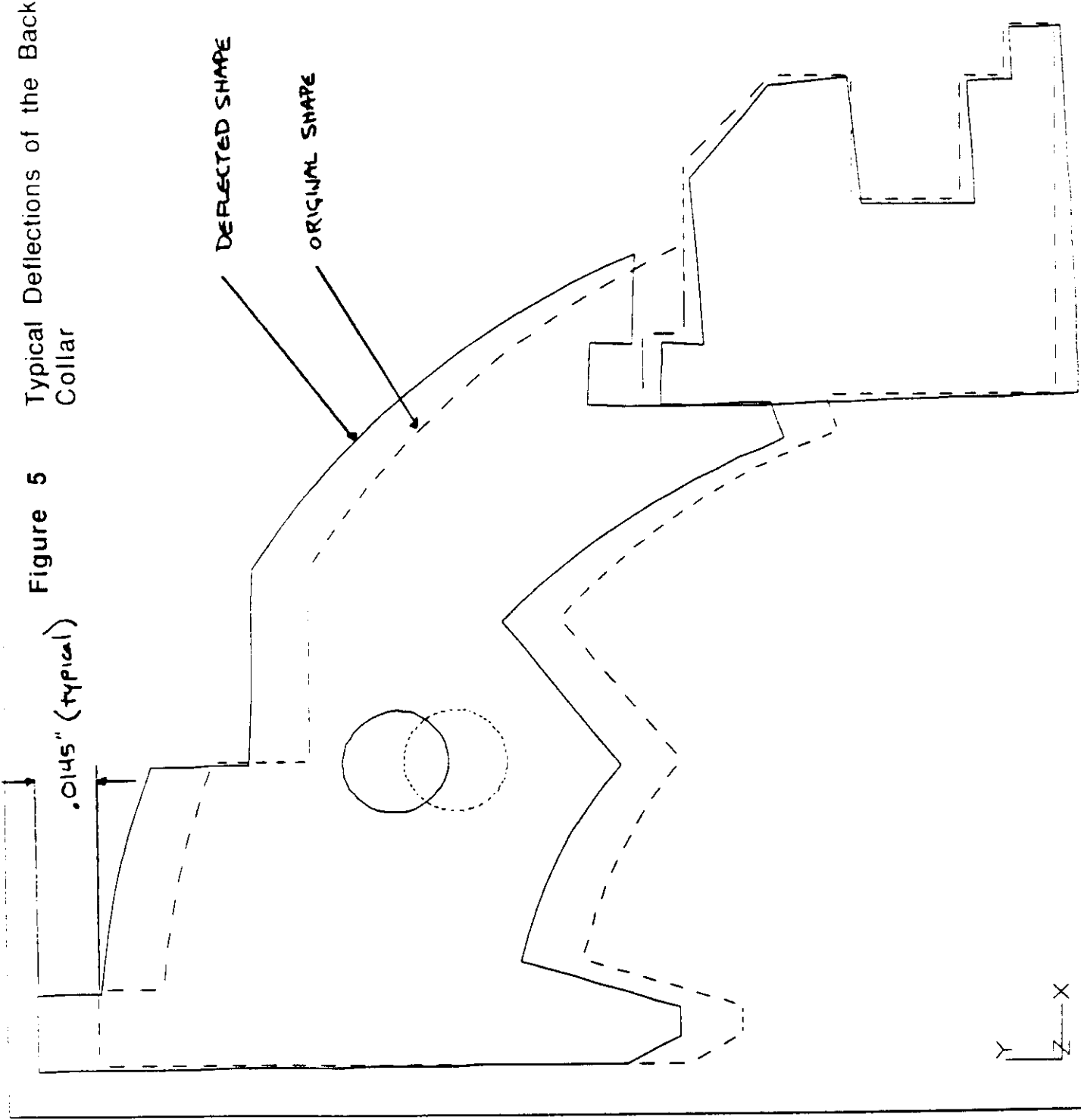
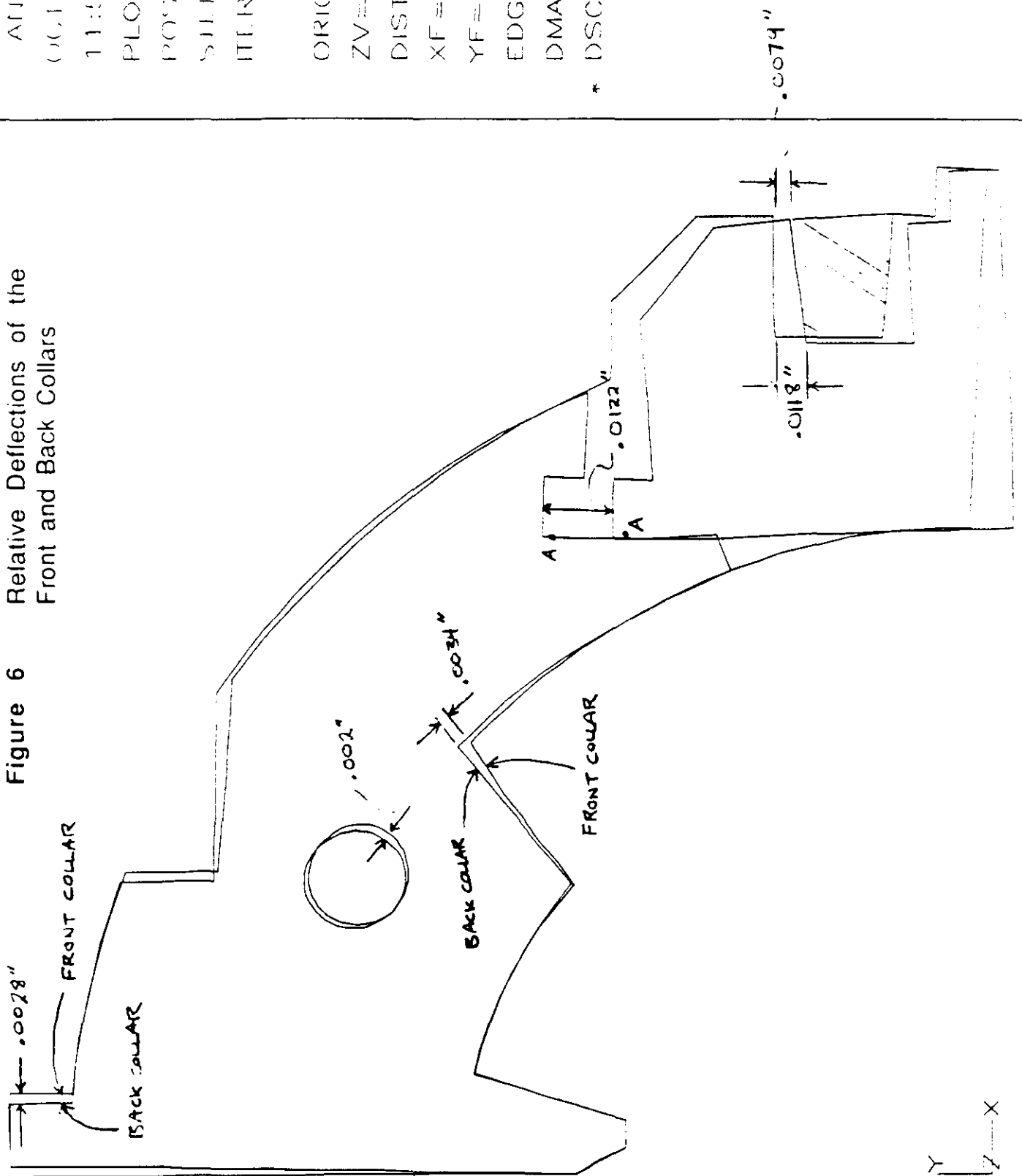


Figure 5 Typical Deflections of the Back Collar

ANALYSIS 4.3
 OCT 6 1988
 9:14:04
 PLOT NO. 3
 POST1 DISPL
 STEP=2
 ITR 15

ORIG
 ZV=1
 DIST=1.39
 XF=1.26
 YF=1.16
 EDGE
 DMAX=.0151
 * DSCA=10

Figure 6 Relative Deflections of the Front and Back Collars



ANSYS 4.5
 06.1 / 1988
 11:50:15
 PLOT NO. 1
 POSIT DISPT
 SLEEP 1
 ITER=15

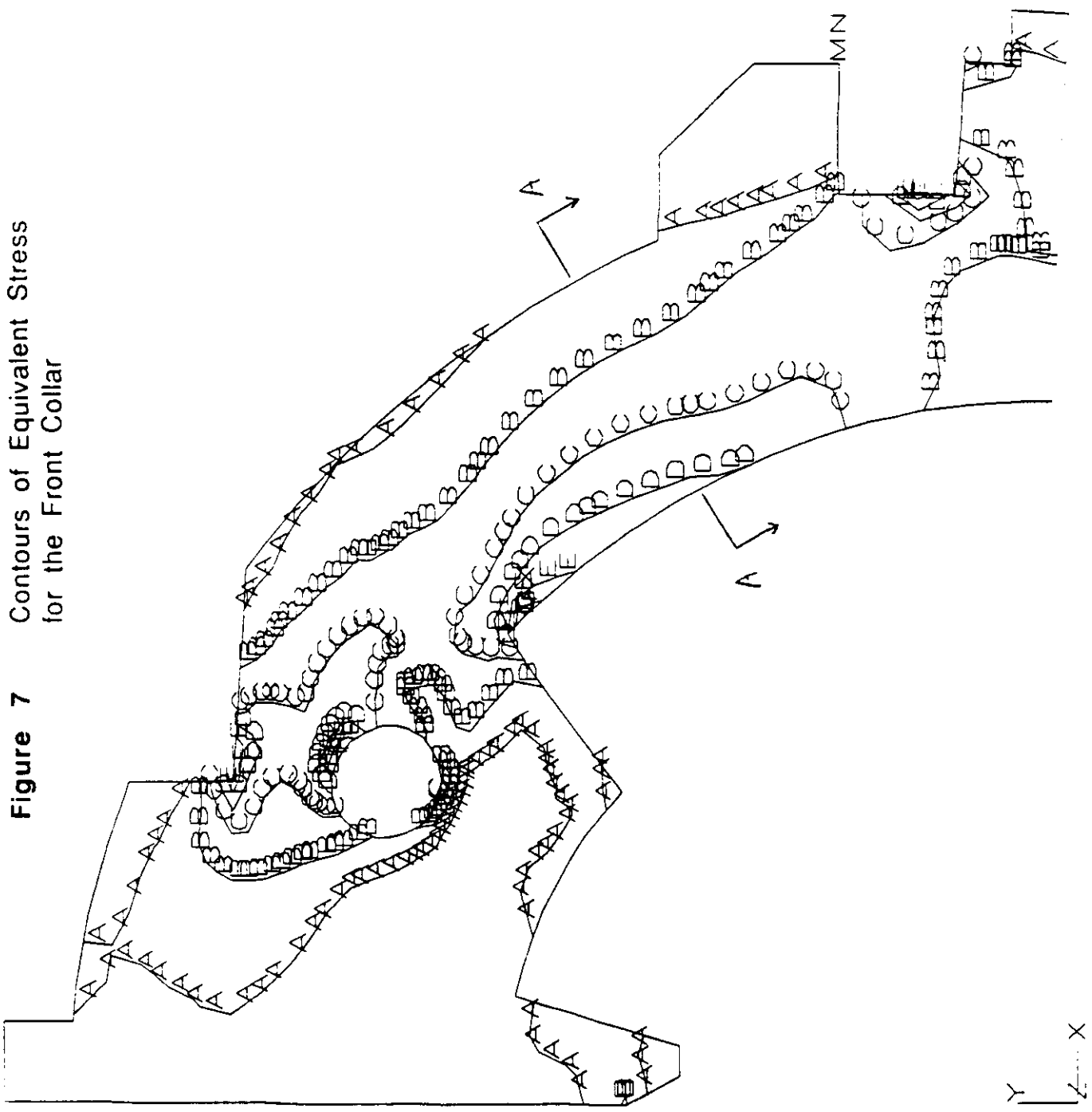
ORIG
 ZV=1
 DIST=1.59
 XF=1.26
 YF=1.16
 EDGE
 DMAX=.0146
 * DSCA= 10

ISSC, NO. 9, MODEL 1 (NOTE: DO NOT SCALE REFLECTIONS)

ANSYS 4.4
 CCI 5 1988
 14:56:03
 PLOT NO. 5
 POST1 STRSS
 STEPS 2
 IITER 15
 SIGE (AVG)

ORIG
 ZV=1
 DIST=1.39
 XF=1.26
 YF=1.16
 F DGT
 MX=73676
 MN=289
 A=10000
 B=20000
 C=30000
 D=40000
 E=50000
 F=60000
 G=70000

Figure 7 Contours of Equivalent Stress for the Front Collar



ANSYS 4.3
 OCT 5 1988
 15:00:13
 PLOT NO. 6
 POST1 STRISS
 STEP=2
 IITER=15
 SIGE (AVG)

ORIG
 ZV=1
 DIST=1.39
 XF=1.26
 YF=1.16
 EDGE
 MX=66896
 MN=25.3
 A=10000
 B=20000
 C=30000
 D=40000
 E=50000
 F=60000

Figure 8 Contours of Equivalent Stress for the Back Collar

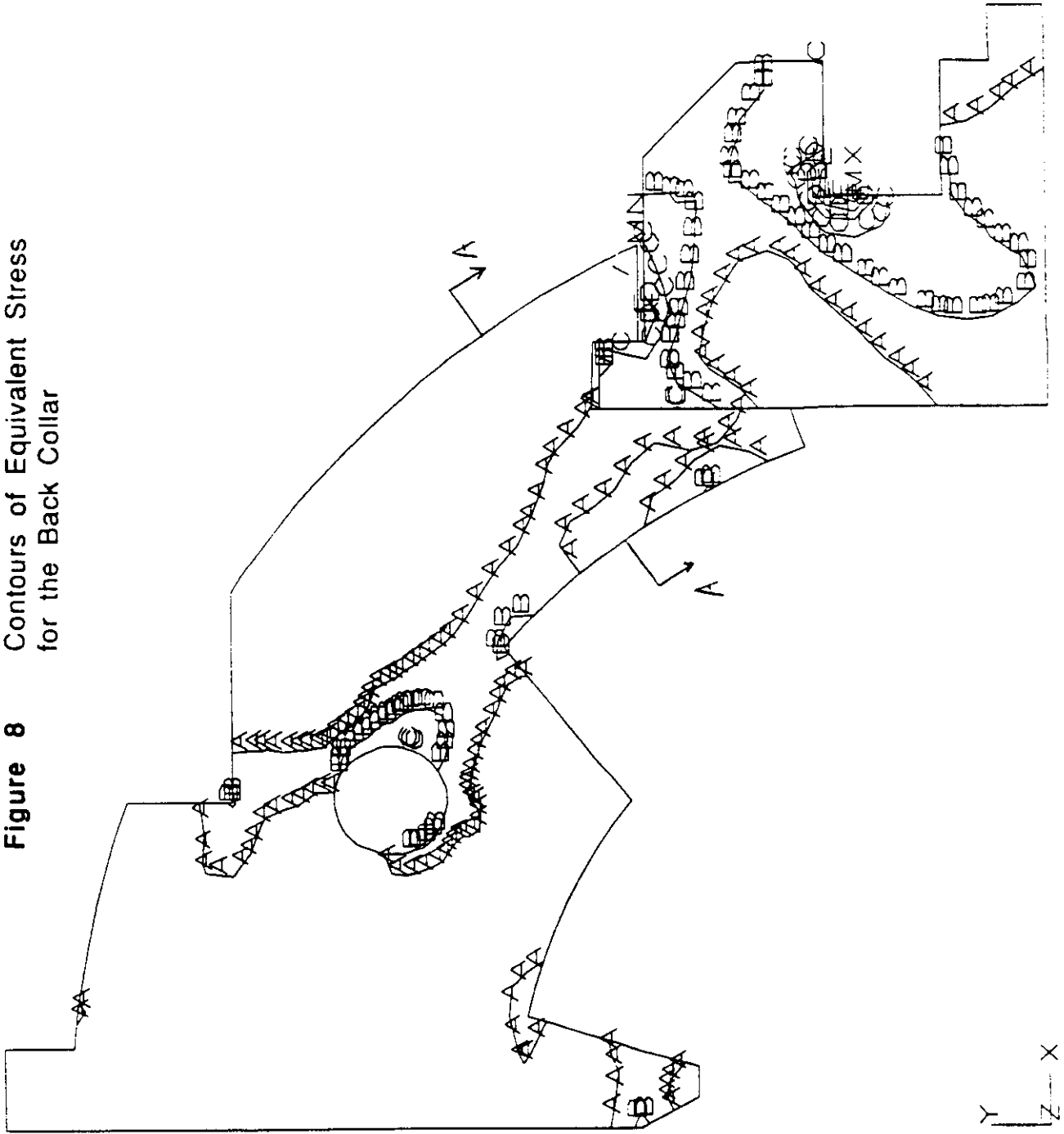
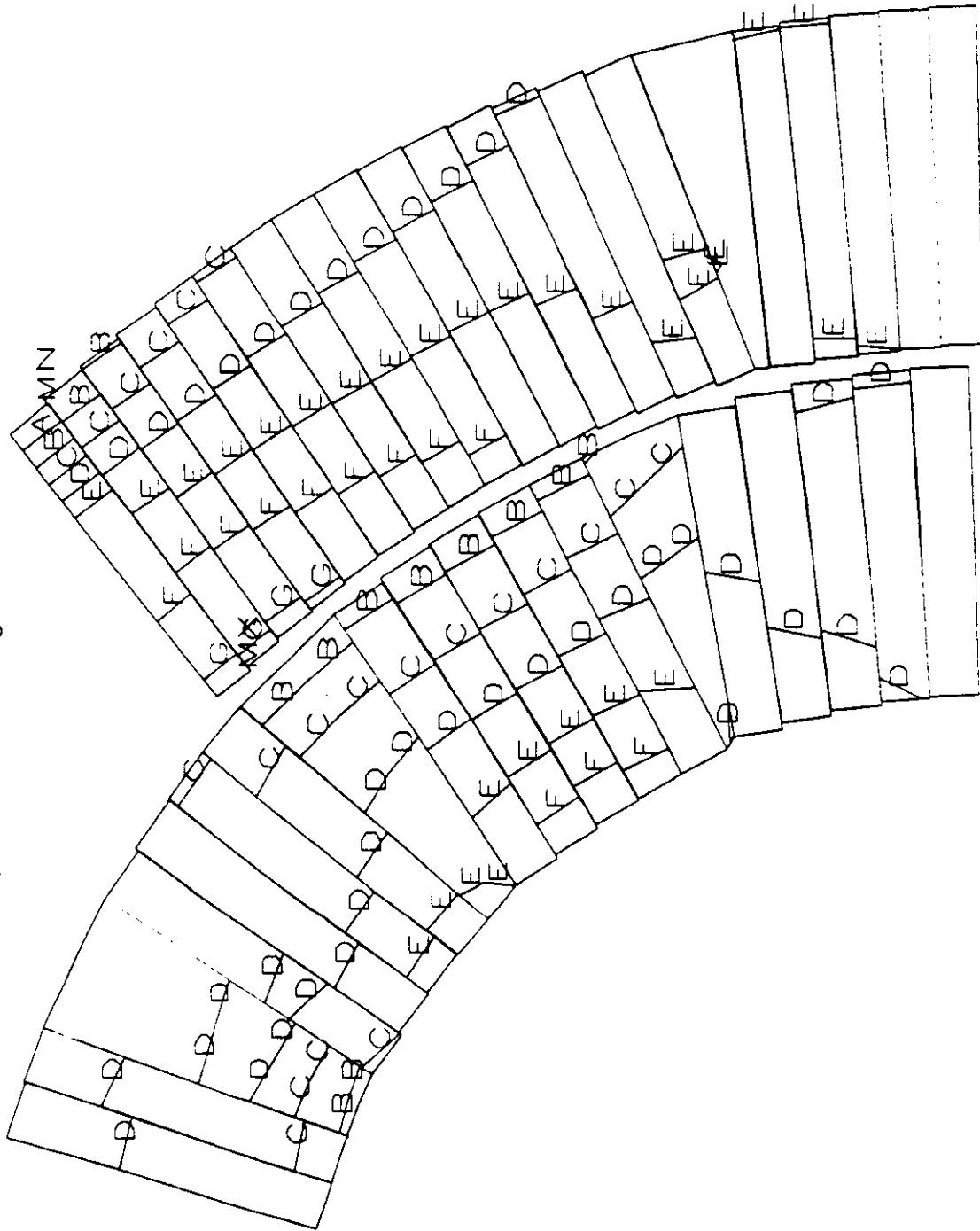
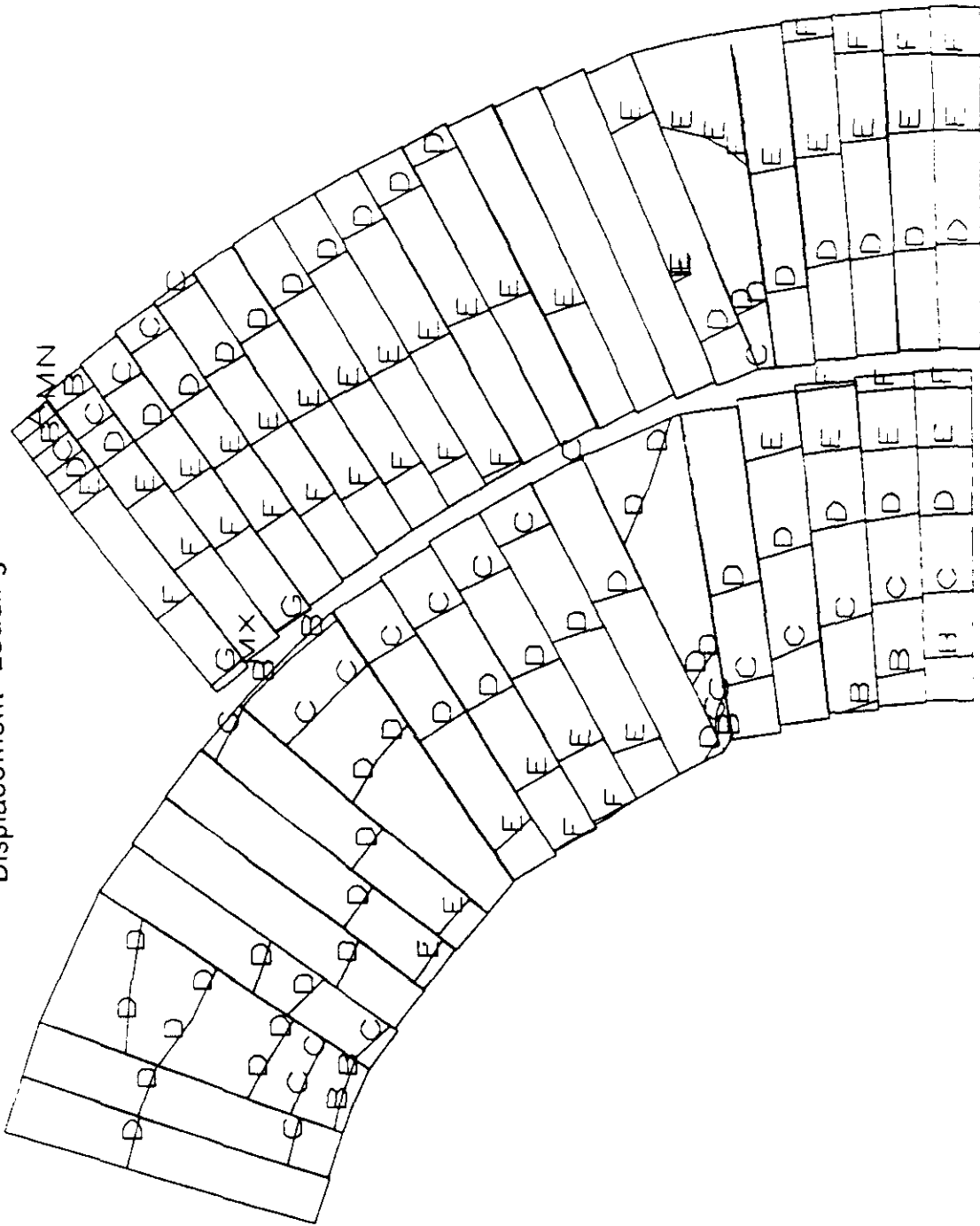


Figure 9 Model 1, Azimuthal Stress
Contours for Uniform Midplane
Pressure Loading



ANALYSIS 4.1.6
 OCL 6 1988
 10:38:24
 PLOT NO. 1
 POST1 STRI55
 STEP=1
 IIR 15
 SY (AVG)
 CSYS=1
 ORIG
 ZV=1
 DIST=.769
 XF=.88
 YF=.571
 EDGE
 MX=-1409
 MN=-16129
 A=-14000
 B=-12000
 C=-10000
 D=-8000
 E=-6000
 F=-4000
 G=-2000

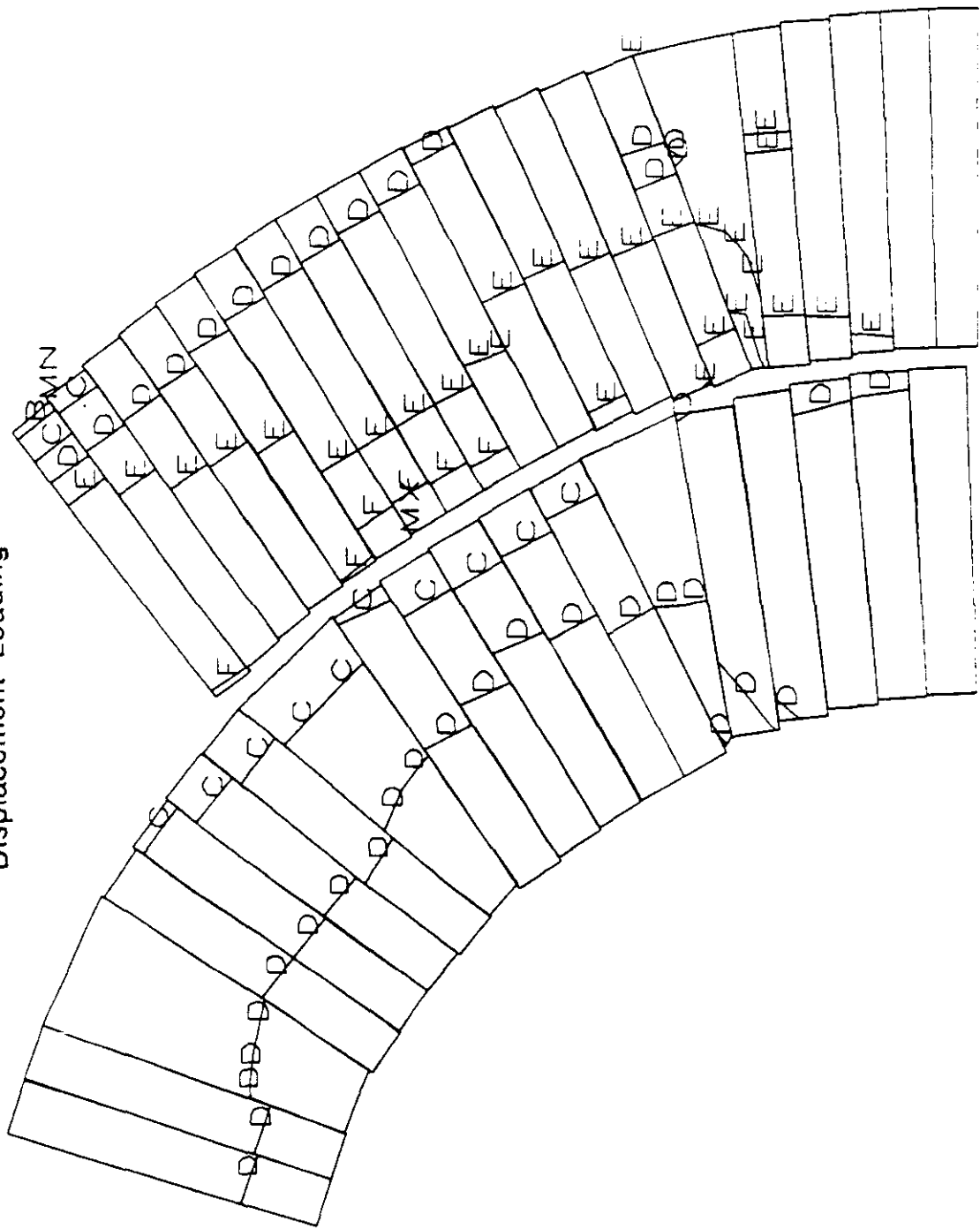
Figure 10 Model 1, Azimuthal Stress
Contours for Uniform Midplane
Displacement Loading



ALLY= 4.5
 OCL 6 1988
 10:29:51
 PLOT NO. 10
 POSIT STRIP=5
 STEP=2
 ITER=15
 SY (AVG)
 CSYS=1

ORIG
 ZV=1
 DIST=.769
 XF=.88
 YF=.571
 EDGI
 MX=-1770
 MN=15410
 A=14000
 B=12000
 C=10000
 D=8000
 E=6000
 F=4000
 G=2000

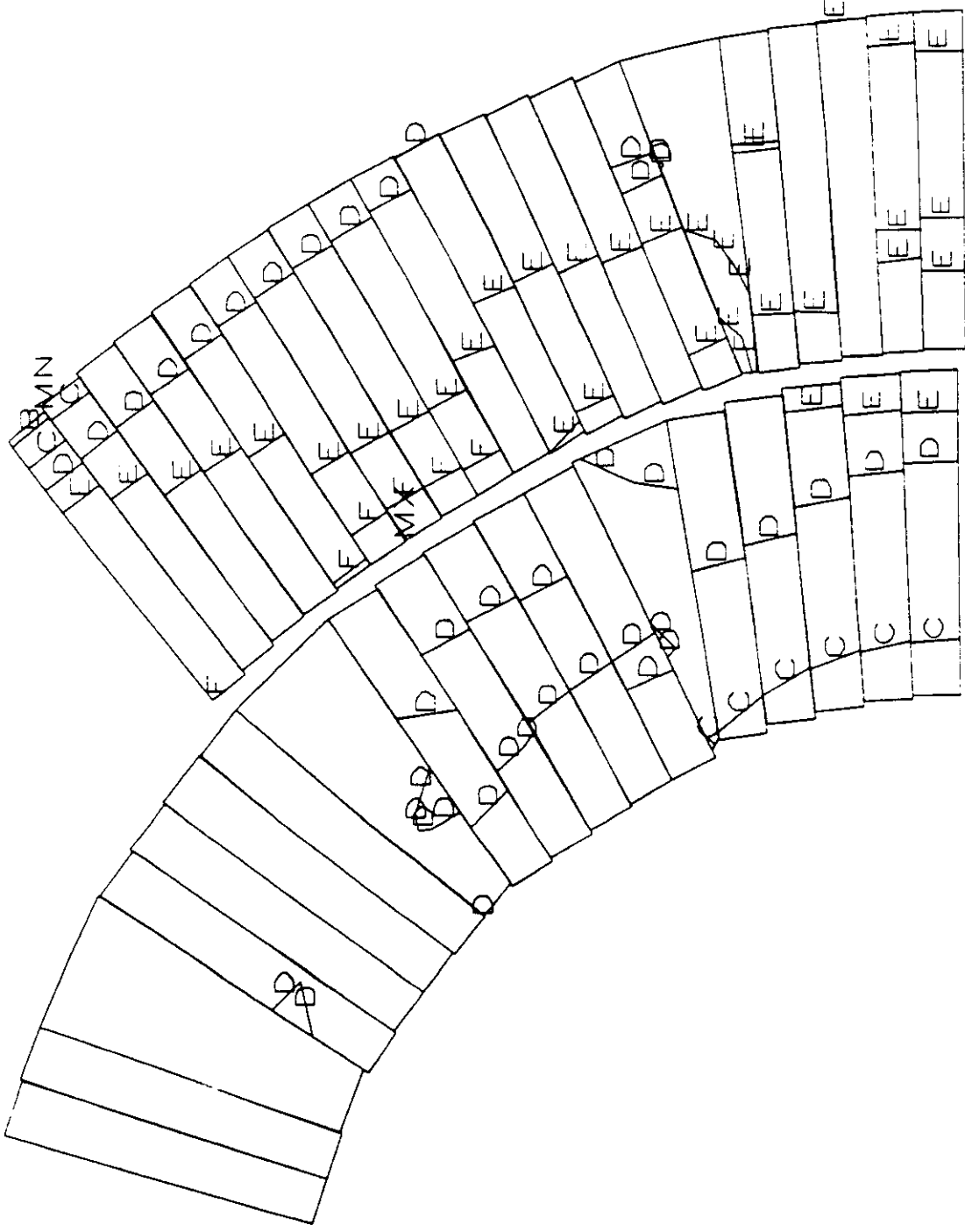
Figure 11 Model 4, Azimuthal Stress
Contours for Uniform Midplane
Displacement Loading



ANSYS 4.5
 OCT 6 1988
 10:41:48
 PLOT NO. 1
 POS11 STRESS
 SHIP=1
 ITER=15
 SY (AVG)
 CSYS=1

ORIG
 ZV=1
 DIST=.769
 XF=.88
 YF=.571
 EDGE
 MX=-2843
 MN=-12695
 B=-12000
 C=-10000
 D=-8000
 E=-6000
 F=-4000

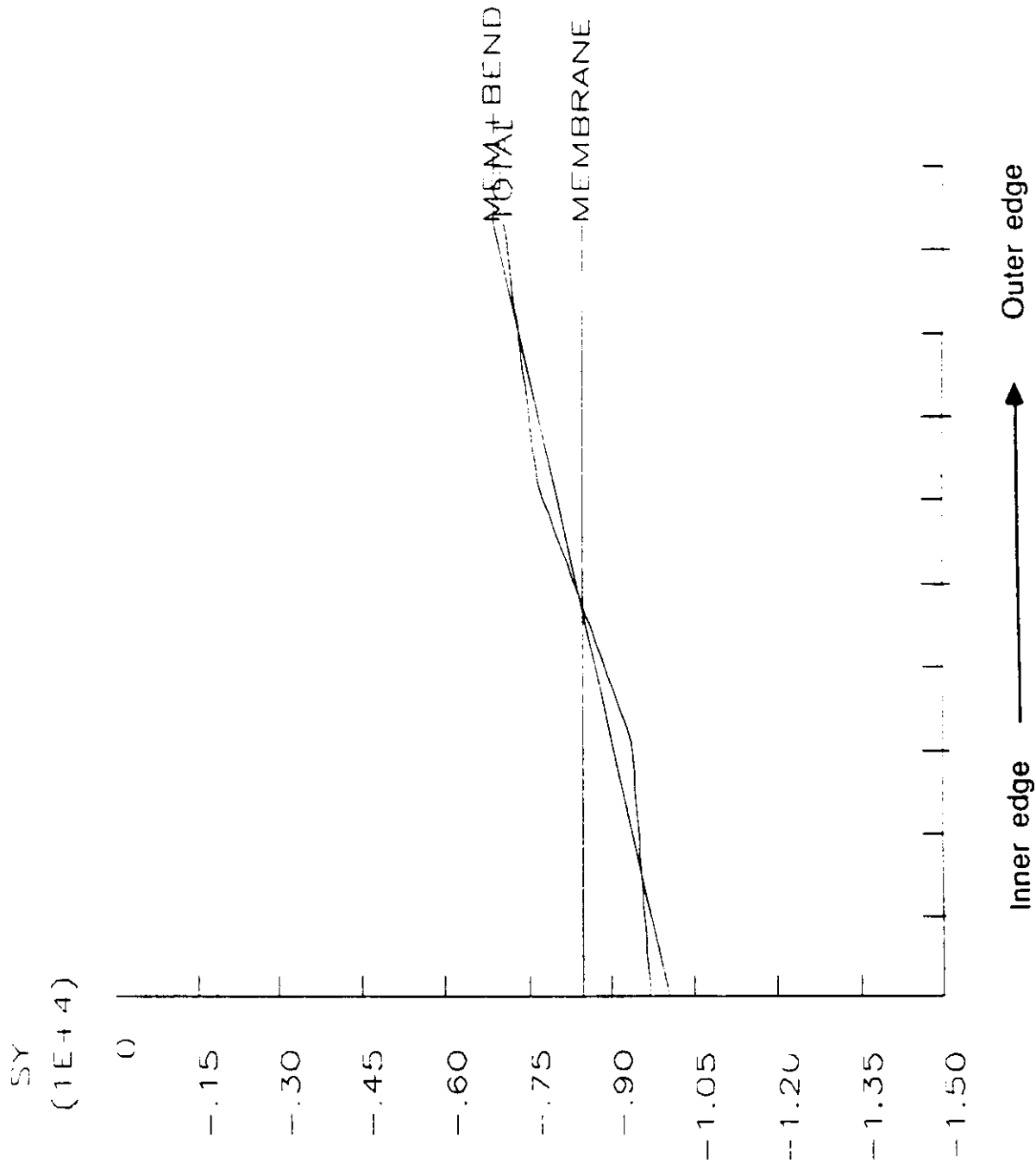
Figure 12 Model 4, Azimuthal Stress
Contours for Uniform Midplane
Displacement Loading



ALP=0.0 4.5
 OCL 6 19888
 10:51:31
 PLOT NO. 1
 POST1 STRI SS
 STEP=2
 ITER=15
 SY (AVG)
 CSYS=1

ORIG
 ZV= 1
 DIST=.769
 XF=.88
 YF=.571
 EDGL
 MX=- 2887
 MN=- 12568
 B= 12000
 C=- 10000
 D=- 8000
 E=- 6000
 F=- 4000

Figure 13 Model 1, Stress Profile Across Inner Coil Pole



ANALYSIS 4.1.5
 DATE 6 1988
 10:29:0.5
 PLOT NO.
 POSIT
 STEP=2
 IITER=15
 SECTION PLOT
 NOD1=149
 NOD2=152
 SY
 CSYS=1
 ORIG
 ZV=1
 DIST=1.41

```

ANSYS  4.3
OCT  6 1988
10:29:51
PLOT NO.  9
      POSH
STEP=2
ITER=15
SECTION PLOT
NOD1=317
NOD2=320
SY
CSYS=1

ORIG
ZV=1
DIST=1.41

```

Figure 14 Model 1, Stress Profile Across Outer Coil Pole

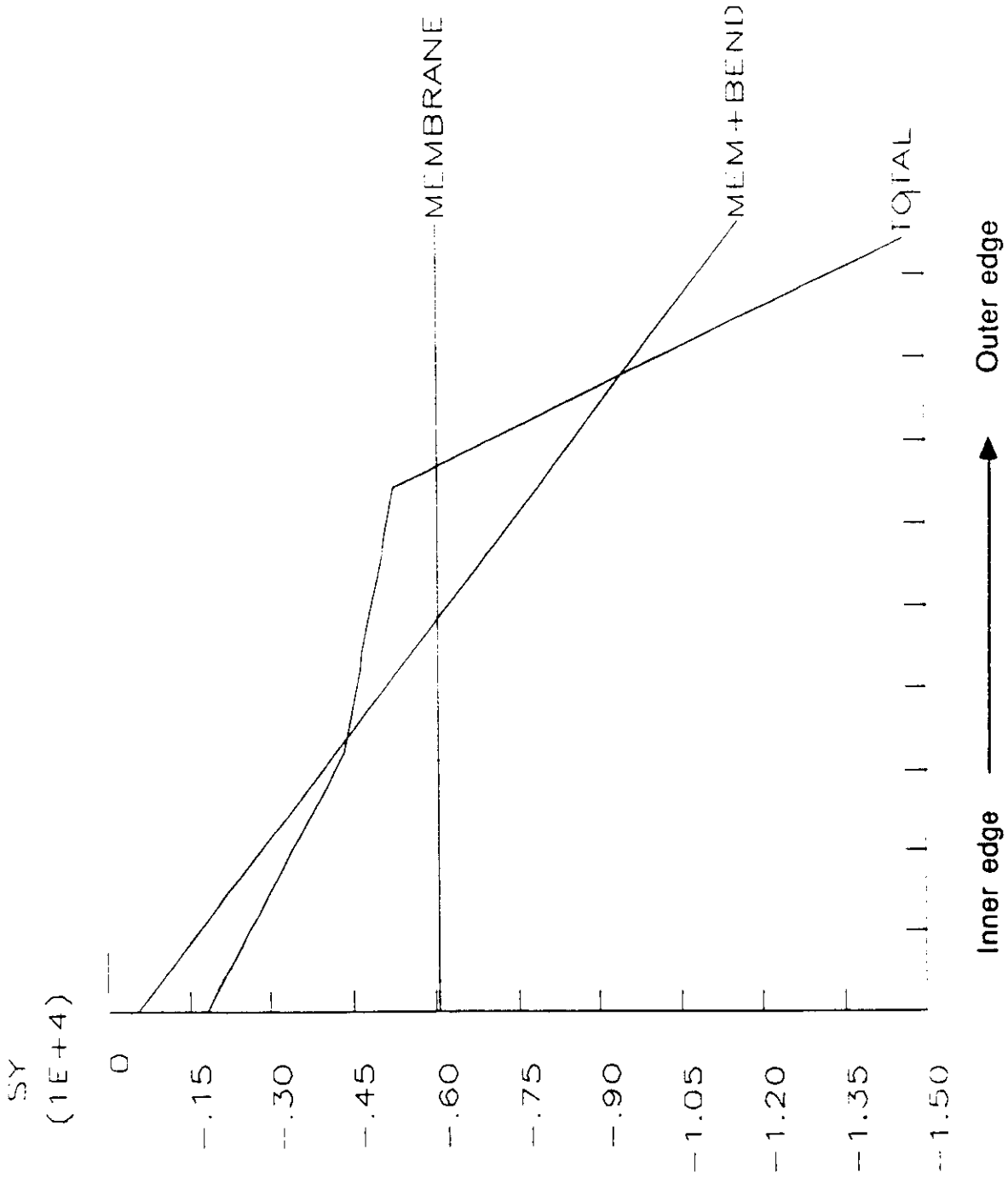
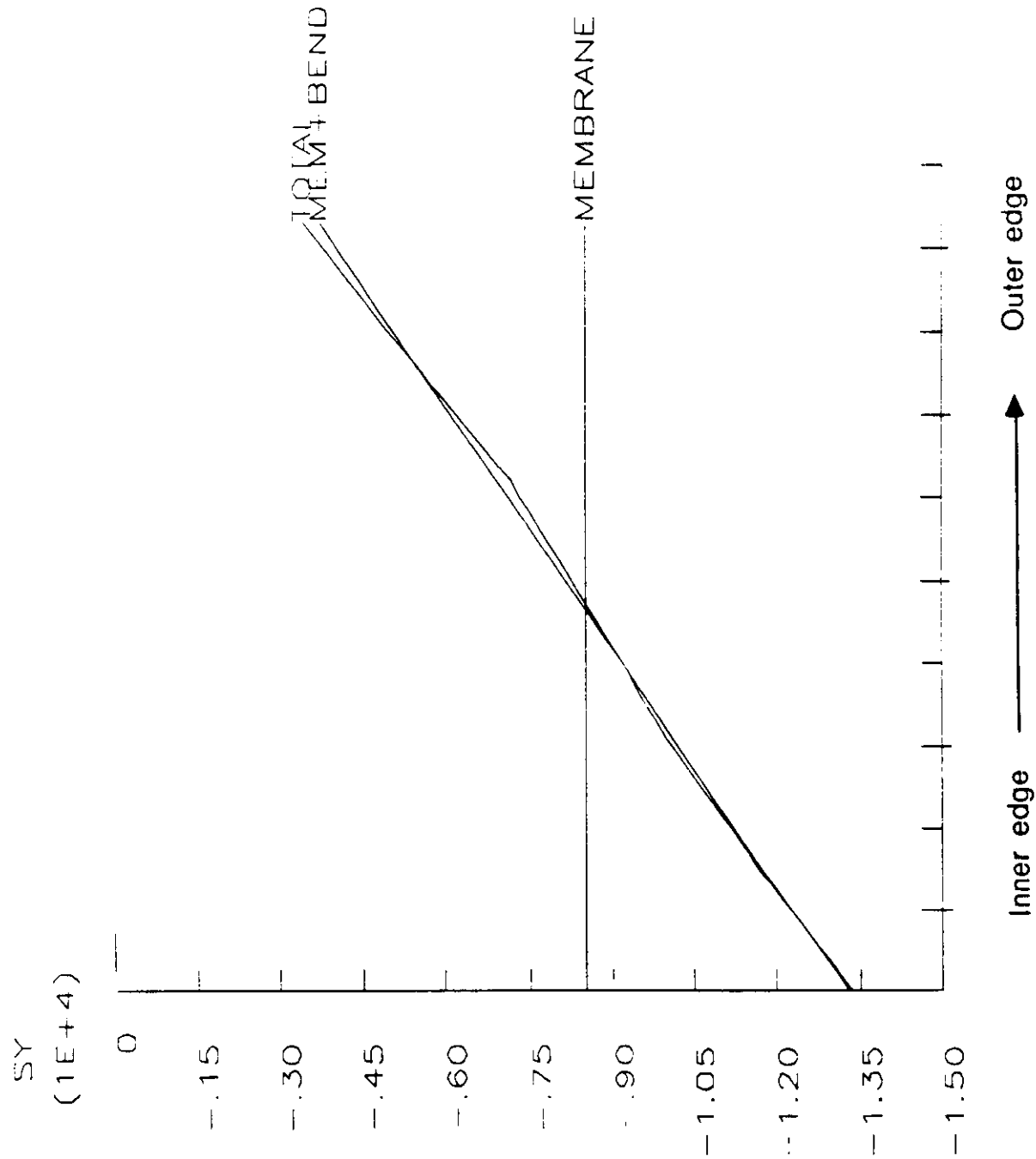
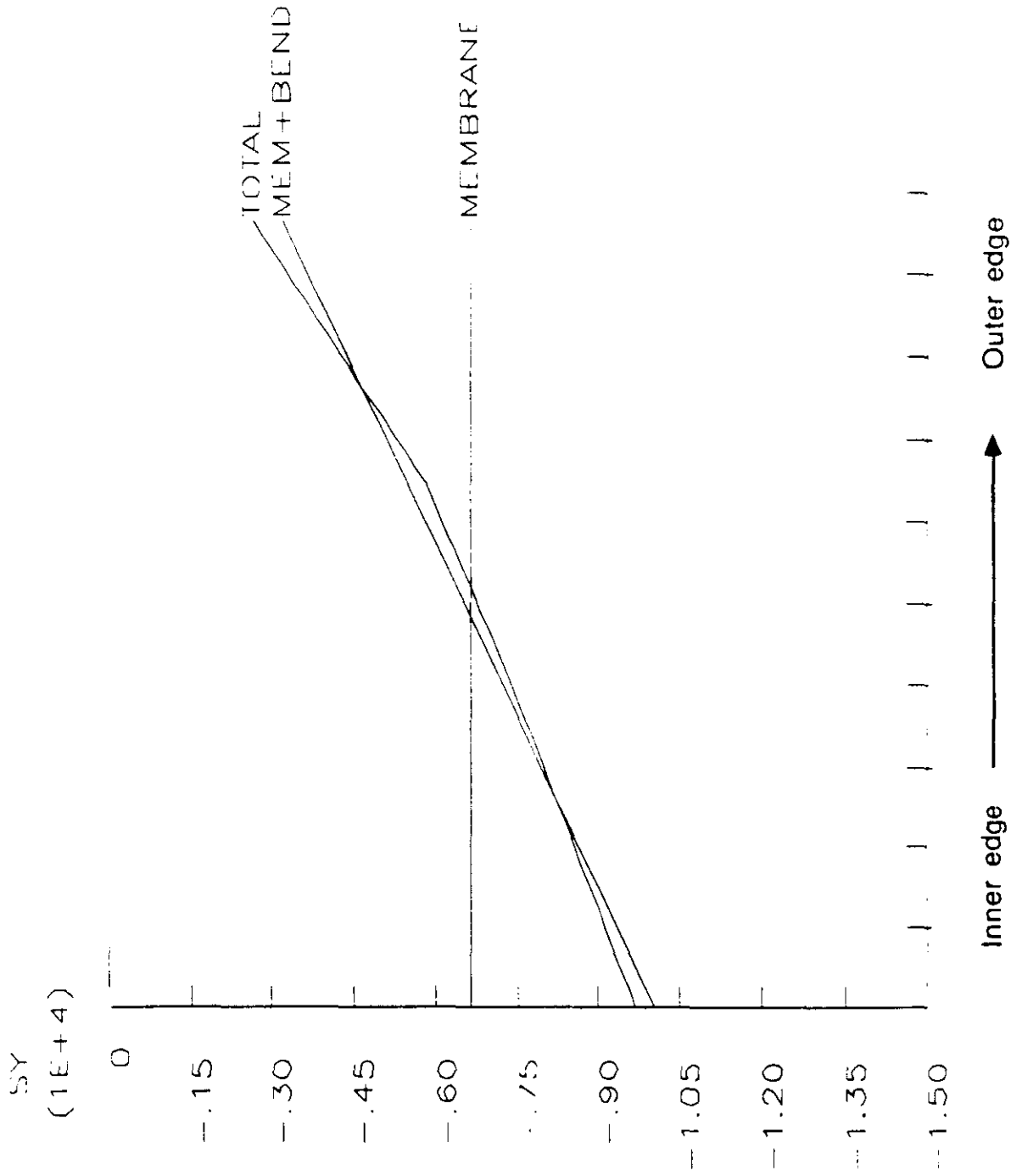


Figure 15 Model 1, Stress Profile Across Inner Coil Midplane



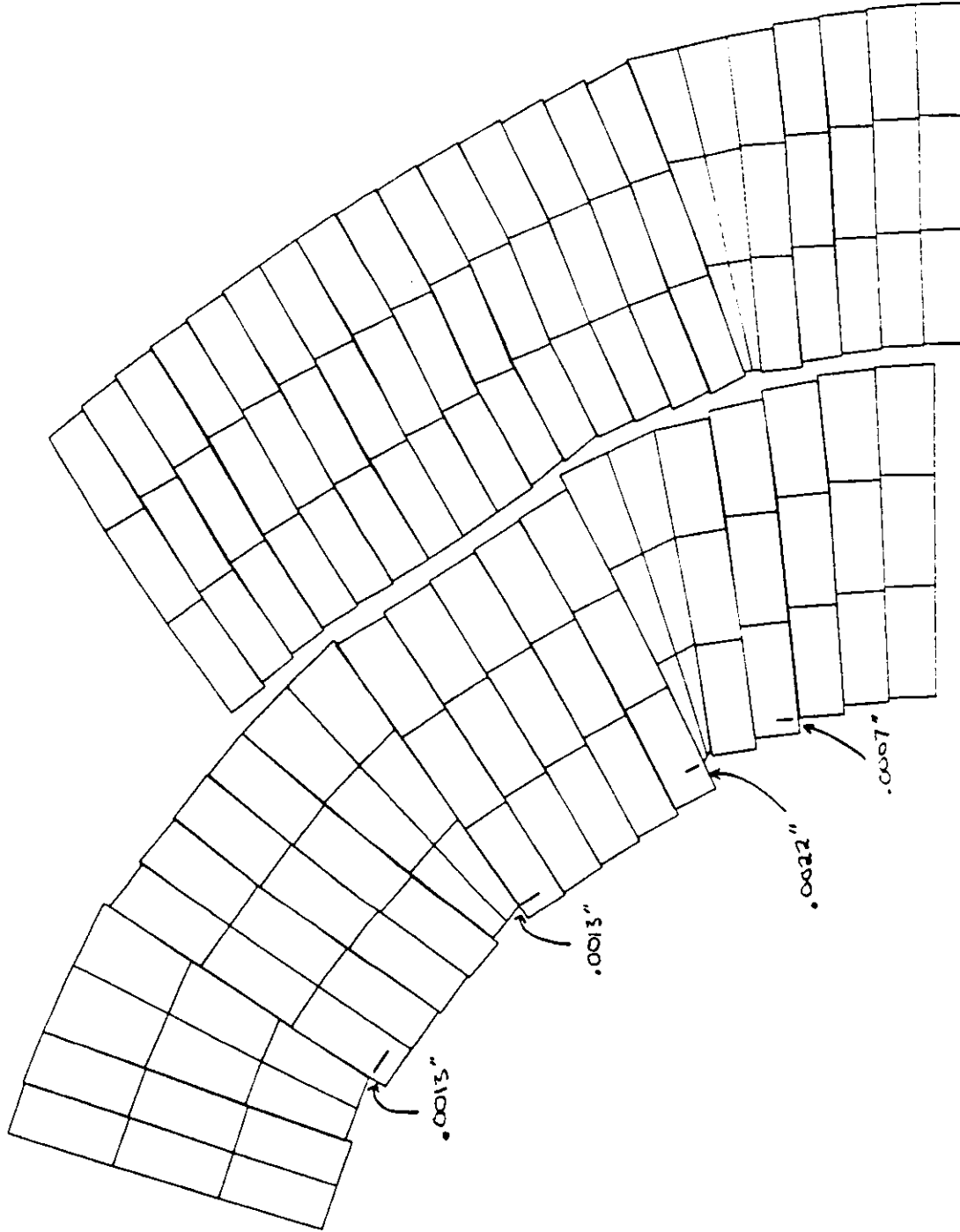
ANSYS 4.3
 OCT 6 1988
 10:28:55
 PLOT NO. 6
 POSIT
 STEP#2
 ITER=15
 SECTION PLOT
 NOD1=1
 NOD2=4
 SY
 CSYS=1
 ORIG
 ZV=1
 DISF 1.41

Figure 16 Model 1, Stress Profile Across
Outer Coil Midplane



ANALYSIS 4.5
 OCT 6 1988
 TIME: 1.5
 PLOT NO. 8
 POSI
 STEP=2
 ITER=15
 SECTION PLOT
 NOD1=155
 NOD2=156
 SY
 CSYS=1
 ORIG
 /V=1
 DIST=1.41

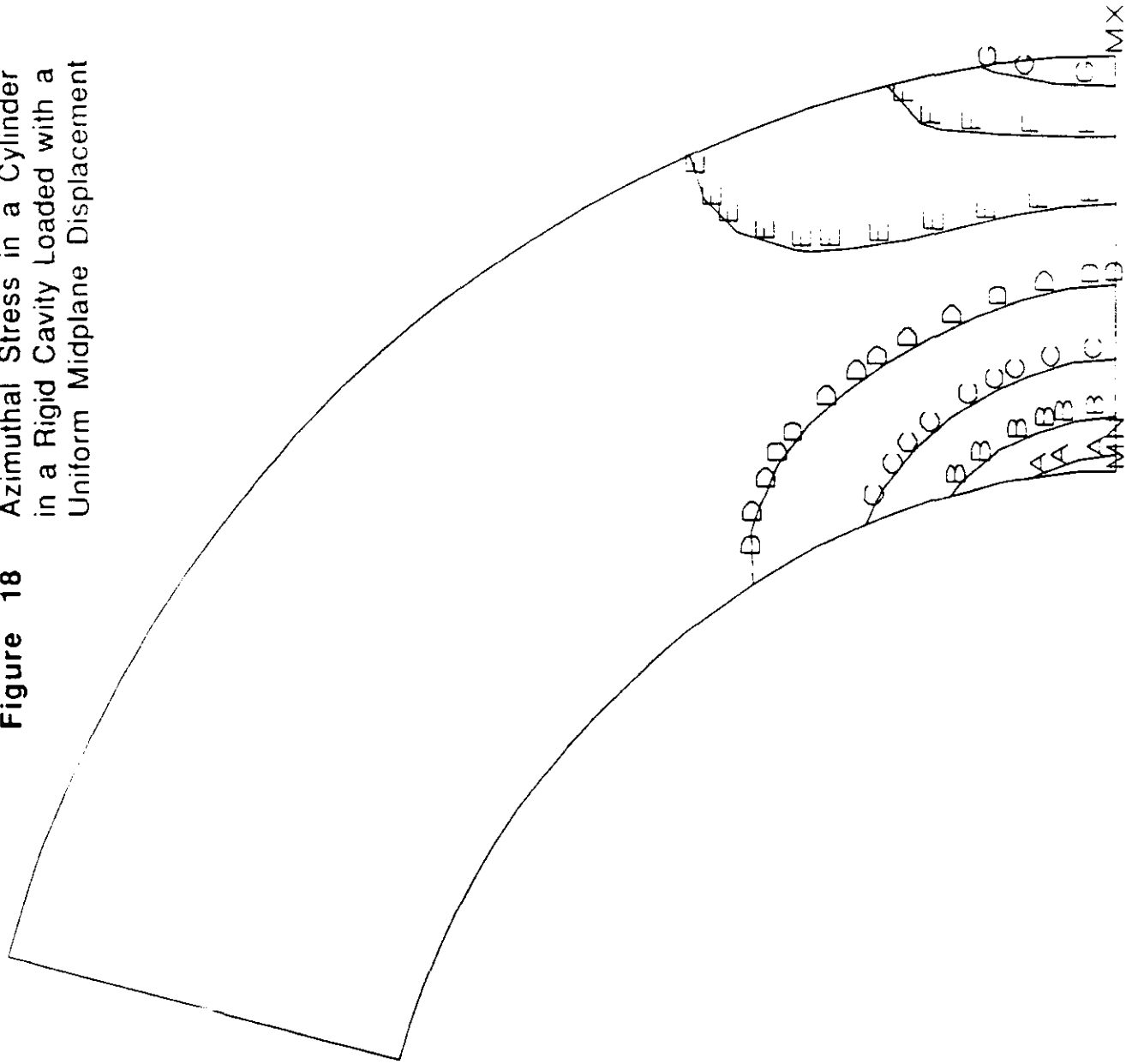
Figure 17 Relative Conductor Motion for Model 4 (conductors free to slide)



ANSYS 4.1.5
 OCT 6 1988
 14:26:18
 PLOT NO. 3
 POS11 DISPL.

STEP=2
 ITER=15
 ORIG
 ZV=.1
 DIST=.769
 * XF=.9
 * YF=.8
 DMAX=.0186
 * DSCA=-15

Figure 18 Azimuthal Stress in a Cylinder in a Rigid Cavity Loaded with a Uniform Midplane Displacement



ANSYS 4.3
 OCL 6 1988
 164109
 PLOT NO. 1
 POINT SERIES
 STEP=1
 ITER=15
 SY (AVG)
 CSYS=1

ORIG
 ZV=1
 DIST=.638
 XF=.704
 YF=.58
 EDGE
 MX= 15.30
 MN= -1585.5
 A= 15000
 B= 13000
 C= 11000
 D= 9000
 E= 7000
 F= 5000
 G= 3000

ANSYS 4.3
 OCT 6 1988
 17:54:49
 PLOT NO. 4
 POST1
 STEP=2
 ITER=15
 PATH PLOT
 NOD1=666
 NOD2=589
 UY
 CSYS=11
 ORIG
 ZV=1
 DIST 1.41

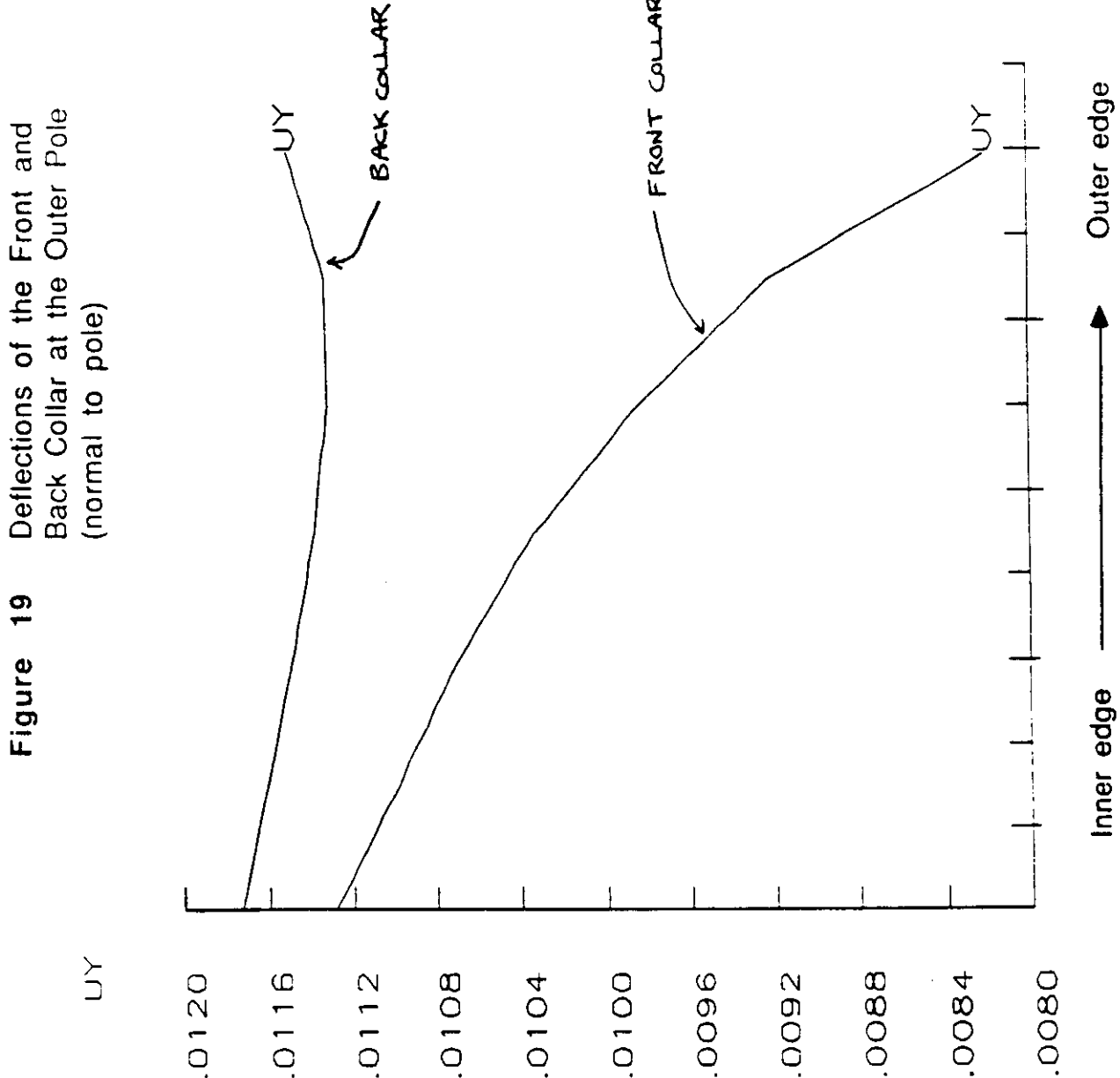
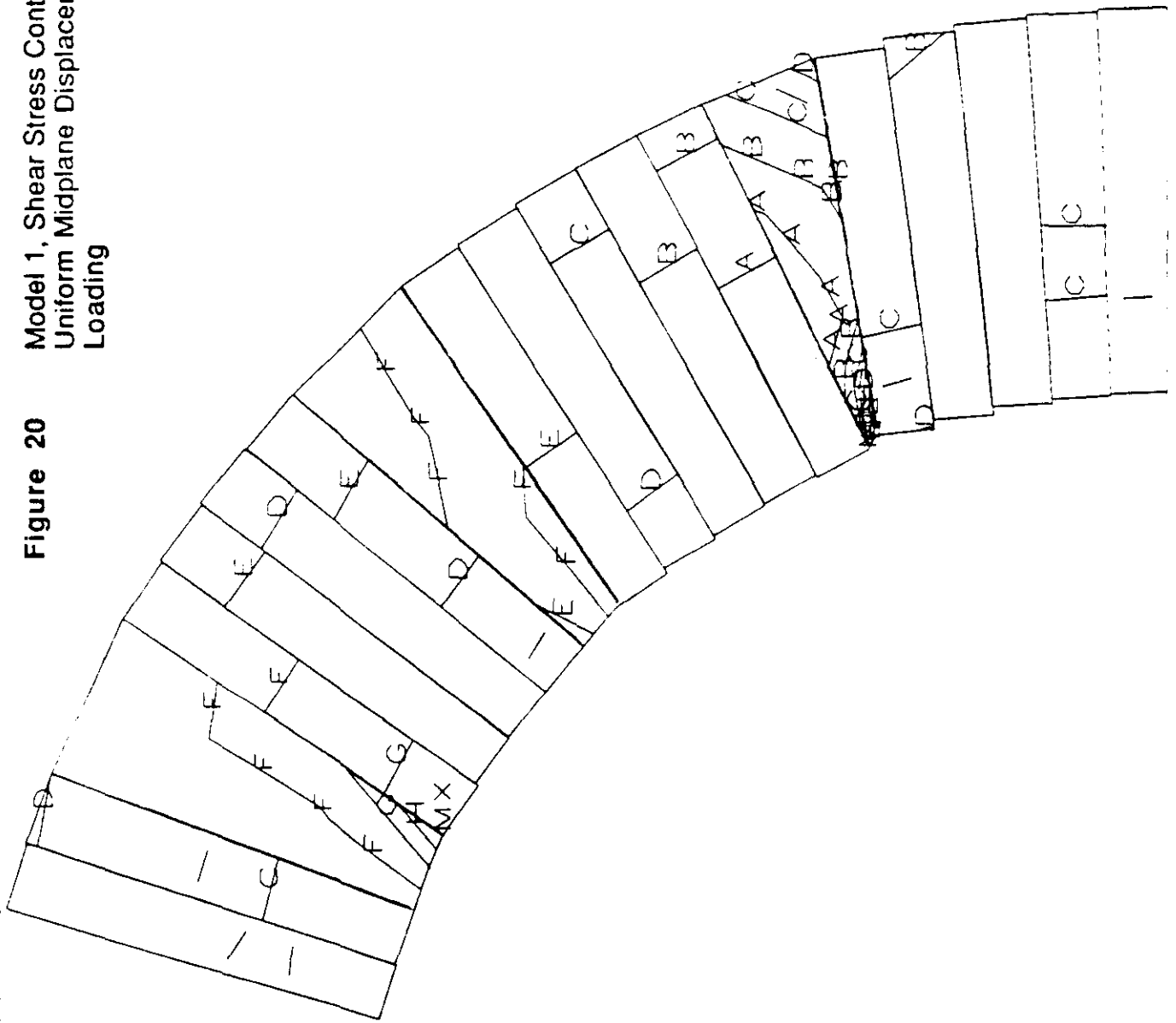


Figure 20 Model 1, Shear Stress Contours for Uniform Midplane Displacement Loading



ANSYS 4.1.5
 OCT 25 1988
 19:19:08
 PLOT NO. 1
 POST1 STRESS
 STEP 2
 IIR 15
 SXY (AVG)
 STRESS ITEM 65

ORIG
 ZV=1
 DIST=.622
 XI=.675
 YI=.569
 EDG1
 MX=.5268
 MN=.2089
 A=1500
 B=900
 C=500
 D=300
 E=900
 F=1500
 G=2100
 H=2700